Yuzuncu Yil University
Journal of the Institute of Natural & Applied Sciences

https://dergipark.org.tr/en/pub/yyufbed

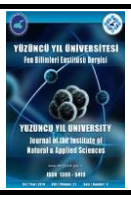

Research Article

Probing the Physics of Molecular Clouds in Spiral Galaxies NGC 5055 and NGC 3627

Hülya ESER SULU[1], Selçuk TOPAL[*2]

[1]Van Yuzuncu Yil University, Institute of Natural and Applied Sciences, Department of Physics, 65080, Van, Türkiye
[2]Van Yuzuncu Yil University, Faculty of Science, Department of Physics, 65080, Van, Türkiye
Hülya ESER SULU, ORCID No: 0000-0002-3187-4208, Selçuk TOPAL, ORCID No: 0000-0003-2132-5632
*Corresponding author e-mail: selcuktopal@yyu.edu.tr

Article Info

Received: 20.09.2023
Accepted: 02.01.2024
Online April 2024

DOI:10.53433/yyufbed.1363547

Keywords
Galaxies,
Molecular clouds,
Spiral galaxies,
Star formation

Abstract: Although galaxies can be grouped in a few categories in terms of morphology, they have remarkably different intrinsic properties. Spiral galaxies host substantial amounts of molecular gas and have ongoing star formation activity with respect to elliptical galaxies lacking star formation. Molecular emission lines are used to probe the internal properties of molecular gas clouds where stars are born and die. Carbon monoxide (CO) is easily detectable in the interstellar medium (ISM) of galaxies. In this research, we probe the physics of the gas clouds at multiple positions in disc galaxies NGC 5055 (M63) and NGC 3627 (M66) using four CO transitions and their line ratios. ^{12}CO(J=1-0) is the brightest across the disc of both galaxies compared to the other lines, i.e., ^{12}CO(J=2-1, J=3-2) and ^{13}CO(J=1-0). The CO intensities show a decrease from the center of the galaxies to the outskirts. However, NGC 3627 shows a rather irregular decrease pattern compared to NGC 5055. The CO line ratios show an increase up to a distance from the center and start to decrease. Although NGC 5055 shows a similar variation in the line ratios on each side of the disc, NGC 3627 has an opposite trend on either side. Therefore, the ISM could have different temperatures, opacity, densities, and levels of star formation in different regions of the galaxy's disc. Our results indicate that the line ratios found at the center of both galaxies are different. The difference could be the result of the bar-driven gas accumulation in the center of NGC 3627. The line ratios in the center of NGC 5055 are within the range found for the centers of other spiral and active galaxies in the literature, but the ratios in the center of NGC 3627 are relatively lower.

NGC 5055 ve NGC 3627 Sarmal Galaksilerinde Molekül Bulutlarının Fiziğinin Araştırılması

Makale Bilgileri

Geliş: 20.09.2023
Kabul: 02.01.2024
Online Nisan 2024

DOI:10.53433/yyufbed.1363547

Öz: Galaksiler morfoloji açısından birkaç kategoride gruplandırılabilse de, oldukça farklı içsel özelliklere sahiptirler. Sarmal galaksiler önemli miktarda moleküler gaz barındırır ve yıldız oluşumu olmayan eliptik galaksilere kıyasla devam eden yıldız oluşum aktivitesine sahiptir. Moleküler ışınım salma çizgileri, yıldızların doğup öldüğü gaz bulutlarının iç özelliklerini incelemek için kullanılır. Karbon monoksit (CO) galaksilerdeki yıldızlararası ortamda (YAO) kolaylıkla tespit edilebilir. Bu çalışmada, dört CO geçişini ve bunların çizgi oranlarını kullanarak NGC 5055 (M63) ve NGC 3627 (M66) disk galaksilerinin birçok bölgesinde gaz bulutunun fiziğini araştırıyoruz. ^{12}CO(J=1-0) geçişi, diğer ^{12}CO(J=2-1, J=3-2) ve ^{13}CO(J=1-

Bu çalışma Doç. Dr. Selçuk Topal'ın danışmanlığında tamamlanan Hülya Eser Sulu'nun yüksek lisans tezinden bazı kısımları içermektedir.

Anahtar Kelimeler
Galaksiler,
Molekül bulutları,
Sarmal galaksiler,
Yıldız oluşumu

0) geçişlerine kıyasla, her iki galaksinin diskinde daha parlaktır. CO akı yoğunlukları galaksi merkezlerinden diskin eteklerine doğru bir azalma göstermektedir. Ancak NGC 3627, NGC 5055'e kıyasla oldukça düzensiz bir azalma eğilimine sahiptir. CO çizgi oranları merkezden uzaklaştıkça bir süre artış gösterir ve daha sonra azalmaya başlar. Her ne kadar NGC 5055 diskinin her iki tarafında çizgi oranları benzer değişim gösterse de, NGC 3627 diskinin her iki tarafında zıt bir değişime sahiptir. Bu nedenle YAO, galaksinin farklı bölgelerinde farklı sıcaklıklara, opaklığa, yoğunluklara ve yıldız oluşum seviyelerine sahip olabilir. Sonuçlarımız, her iki galaksinin merkezinde bulunan çizgi oranlarının farklı olduğunu göstermektedir. Bu fark, NGC 3627'nin merkezi bölgesinde çubuk yapısı nedeniyle oluşan gaz birikiminin bir sonucu olabilir. NGC 5055'in merkezindeki çizgi oranları literatürdeki diğer sarmal ve aktif galaksilerin merkezleri için bulunan aralıktadır, ancak NGC 3627'nin merkezindeki oranlar nispeten daha düşüktür.

1. Introduction

There are many types of galaxies in the observable universe with their own physical and dynamic structures (Hubble, 1936; de Vaucouleurs, 1974; de Vaucouleurs et al., 1991; Cappellari et al., 2011; Kormendy & Bender, 2012). Spiral galaxies host substantial cold gas reservoirs, i.e., the fuel for star formation, and show substantial star formation activity. The interstellar medium (ISM) of galaxies has a dynamic and complex structure consisting of many phenomena at play, such as stellar birth and death, supernova explosions, stellar winds, turbulence, and cosmic rays, all affecting the physics and chemistry of the medium (Maloney et al., 1996; Fukui et al., 2009; Padovani et al., 2009). The environment's atomic, ionized, and molecular structure can be studied using different tracers, such as carbon monoxide (CO). The CO is very abundant in spiral galaxies and is widely used to study star-forming gas clouds (Weinreb et al., 1963; McKee & Hollenbach, 1980; Hollenbach & Tielens, 1999; Saintonge & Catinella, 2022 and references therein). The CO line is the most used tracer among more than 300 molecules detected in the ISM or circumstellar shells (Endres et al., 2016), and its low-*J* rotational transitions are easily detectable from the ground.

The change in the line ratios in galaxies could depend on many factors, such as the position over the disc, galaxy types, and local star formation processes. Papadopoulos & Seaquist (1998) obtained an average value of ^{12}CO(2-1) / ^{12}CO(1-0) = 0.70 and ^{12}CO(1-0) / ^{13}CO(1-0) = 11.7 for a sample of Seyfert galaxies. Paglione et al. (2001) studied 17 nearby spiral galaxies and found that the ratio between ^{12}CO(1-0) and its isotopologue ^{13}CO(1-0) decreased with radius from the center. This indicates an increase in the CO-to-H_2 conversion factor, X_{CO}, from the center to the outskirts. Israel (2020) studied the center of spirals and found a large range for the same ratio, i.e. the ratio varies from 5 to 30.
Leroy et al. (2009) studied nearby spirals and found that the ^{12}CO(2-1) / ^{12}CO(1-0) ratio varies from 0.6 to 1.0 across the disc, similar to the ratios found in the Milky Way, and the ratio tends to get higher in the center.

In this study, we targeted two spiral galaxies, i.e., NGC 5055 (Messier 63 or M63) and NGC 3627 (Messier 66 or M66), having different disc morphologies (i.e., galaxies with and without a dominant central bar structure) and different nuclear activities (i.e., galaxies with and without an active galactic nucleus, AGN) to study the line ratios in the center and across the disc of spiral galaxies. This will allow us to investigate the line ratios' dependence on the environment and galaxy morphology.

NGC 5055 and NGC 3627 are rich in molecular gas and had multiple CO lines detected. NGC 5055 and NGC 3627 are nearby spiral galaxies located at a distance of 9 and 11.5 Mpc, respectively (NASA Extragalactic Database, NED). NGC 3627 is an S3-type Seyfert galaxy hosting an active galactic nucleus (AGN) and a bar at its center. NGC 5055 is however a non-barred galaxy and does not show an AGN activity (NED). Our goals are to explore the physics of molecular gas clouds across the radial cut of both galaxies using multiple CO line ratios such as temperature, density, and opacity and to compare our results with the literature studies done for different galaxies.

Table 1. Basic properties of NGC 5055 and NGC 3627

Property	NGC 5055	NGC 3627	Reference
Galaxy type	SA(rs)bc	SAB(s)b, S3	a
RA (J2000)	$13^h15^m49.33^s$	$11^h20^m14.96^s$	a
DEC (J2000)	+42°01'45.4"	+12°59'29.54"	a
Major axis diameter (arcminutes)	3.4	3.1	a
Minor axis diameter (arcminutes)	1.9	1.7	a
$V_\odot$ (km/s)	500	720	a
Distance (Mpc)	9.0	11.5	b
Position angle (degree)	103	168	b
Inclination (degree)	55	67.5	b

[a]Nasa/Ipac Extragalactic Database (NED), [b]HyperLEDA (Makarov et al., 2014).

Our paper is set up as follows. In Section 2, we present the data and analysis methods. We present our results and make related discussions in Section 3. Finally, we briefly make our final remarks in Section 4.

2. Material and Methods

2.1. The CO data

Literature CO data for both galaxies in our sample were taken from various sources. The data of ^{12}CO(1-0) and ^{13}CO(1-0) were taken from the CO Multi-line Imaging of Nearby Galaxies (COMING, Sorai et al., 2019), while ^{12}CO(2-1) and ^{12}CO(3-2) data were taken from the Hera CO Line Extragalactic Survey (HERACLES; Leroy et al., 2009), and from the James Clerk Maxwell Telescope (JCMT) Nearby Galaxies Legacy Survey (JCMT NGLS; Wilson et al., 2012), respectively. Four low-*J* CO lines were obtained for both galaxies, i.e. ^{12}CO(1-0), ^{12}CO(2-1), ^{12}CO(3-2), and ^{13}CO(1-0). Each CO data has a different angular resolution, i.e., 17, 11, and 14.5 arcseconds (arcsecs) for ^{12}CO(1-0), ^{12}CO(2-1), and ^{12}CO(3-2), respectively.

Table 2. The basic properties of CO data for galaxies NGC 5055 and NGC 3627

Transition	Frequency (GHz)	Telescope	Beam size (")	Linear size (kpc)	Source
^{12}CO(1-0)	115.27	Nobeyama 45m	17	0.8	Sorai et al., 2019
^{13}CO(1-0)	110.20	Nobeyama 45m	17	0.8	Sorai et al., 2019
^{12}CO(2-1)	230.53	IRAM 30m	11	0.5	Leroy et al., 2009
^{12}CO(3-2)	345.79	JCMT 15m	14.5	0.7	Wilson et al., 2012

2.2. Analysis

2.2.1. Moment maps

The total CO intensity map for both galaxies NGC 5055, and NGC 3627 (hereafter moment 0) was created using the MIRIAD, Multichannel Image Reconstruction, Image Analysis, and Display (Sault et al., 1995) package. The unit in the maps is K km s^{-1}, where K stands for Kelvin. We defined an area for the total CO intensity by following the procedure described in a previous paper (Topal et al., 2016). The moment 0 maps are shown in Figure 1.

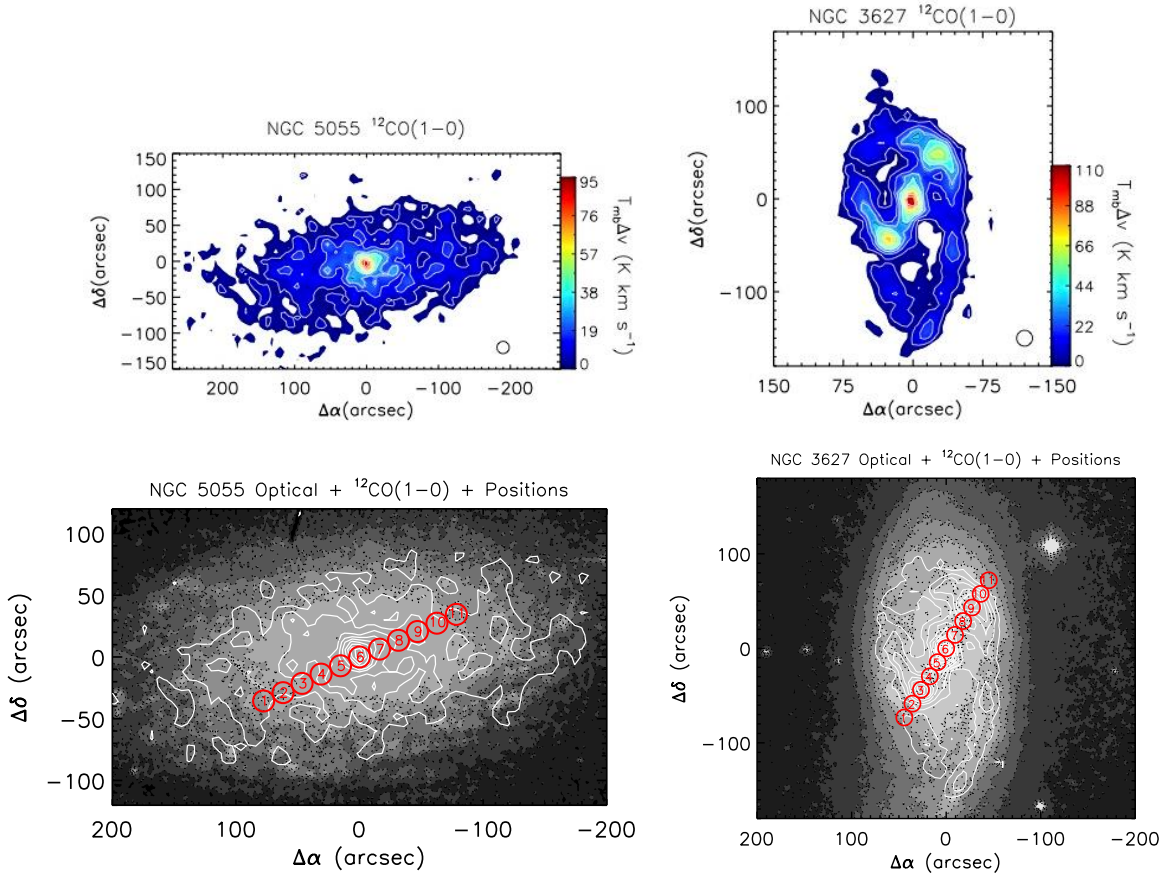

Figure 1. Top: The total ^{12}CO(1-0) integrated intensity maps (moment 0) for both galaxies are shown. The black circles in the top panels indicate the angular resolution. The contour levels on the maps are indicated by white lines, each separated by 10 percent of the peak intensity. The peak ^{12}CO(1-0) intensities are 95.4 K kms^{-1} and 110.1 K kms^{-1} for NGC 5055 and NGC 3627, respectively. Bottom: The selected positions are indicated by red circles over the galaxies. Each red circle has a diameter of 17 arcsecs, equivalently a linear size of about 0.8 kpc over each galaxy. The CO intensity maps (white contours) are overlaid on the Sloan Digital Sky Survey image of the galaxies (grey contours on the background).

2.2.2. Total integrated intensities

A total of 11 circular positions, each having an angular diameter of 17 arcsecs, were chosen over the major axis of the galaxies (see Figure 1). The beam-averaged CO spectra were extracted from each position, and then a Gaussian fit was applied using the Interactive Data Language (IDL) package (see Section 2.2.1). We fit a single Gaussian function (see Eq. 1) to all CO spectra to calculate the total integrated intensities at the selected positions over the galaxy's major axis. The Gaussian function is given below.

$$f(v) = Ae^{\frac{-(v-v_0)^2}{2\sigma^2}} \quad (1)$$

where A is the peak flux at the v_0, i.e., the velocity at the center, and σ is the profile width (root-mean-square velocity), i.e., FWHM $= 2\sqrt{2ln2}\,\sigma = 2.354\,\sigma$, where the FWHM is the Full Width at Half Maximum. An IDL code MPFIT was performed to optimize the fit (Markwardt, 2009). We increased the optimization by running MPFIT many times using different ranges for the fit parameters instead of considering one initial set of values for the fit. As a final step, the chi-square was calculated for the fitting parameters. The parameters with the smallest reduced chi-squared value ($\Delta\chi^2 = \chi^2 - \chi^2_{min}$) were defined as the best fit.

The ^{12}CO(1-0), ^{13}CO(1-0) , ^{12}CO(2-1) and ^{12}CO(3-2) spectra obtained at the center (i.e., position 6, see Figure 1) are given as an example below (Figure 2). At some positions in both galaxies, ^{13}CO(1-0) was not detected due to low signal-to-noise (i.e., S/N < 3), and ^{12}CO(1-0) was not detected at one position in NGC 3627, i.e., the position 11 (see Figure 1). We, therefore, calculated an upper limit, (i.e., the maximum intensity possible given the noise, velocity resolution, and line width), for the CO intensities at those positions using $3 \times \sigma_{rms} \times \delta v \times \sqrt{N}$, where σ_{rms} is the rms noise, δv is the velocity resolution of 10 km/s, and N represents the number of velocity channels covering the line emission. The upper limit CO intensities are shown with an arrow in Figure 3.

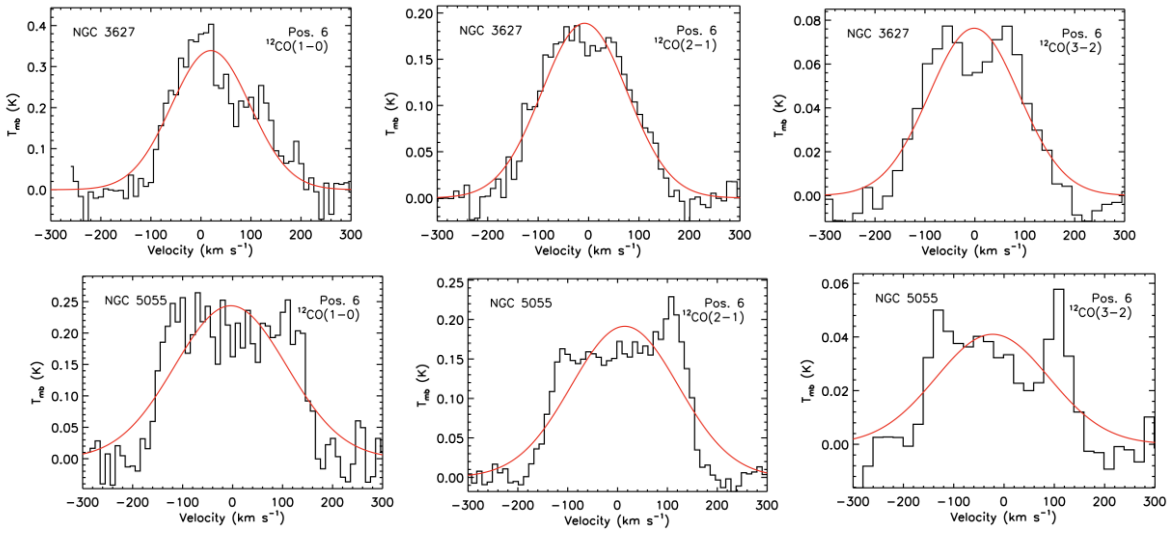

Figure 2. The spectra of the ^{12}CO(1-0, 2-1, 3-2) lines detected at the center of the galaxies NGC 5055 (top) and NGC 3627 (bottom) are shown as an example. The solid red line indicates the best-fit Gaussian function.

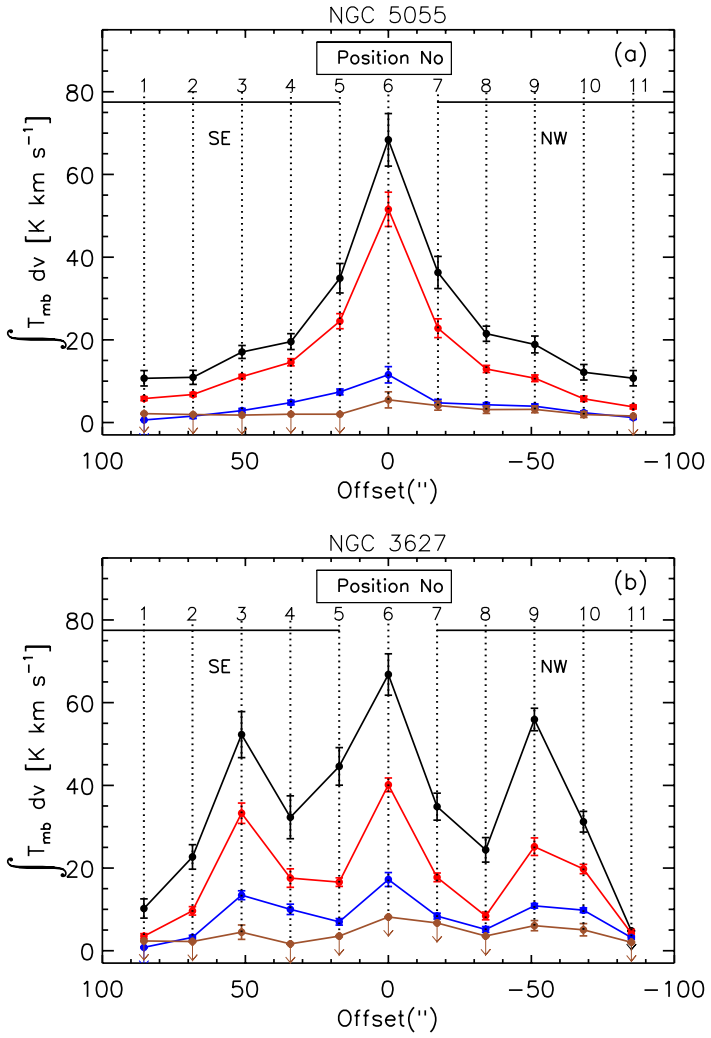

Figure 3. The total CO integrated intensities calculated over the disc of NGC 5055 (panel a) and NGC 3627 (panel b) are shown, respectively. The ^{12}CO(1-0), ^{12}CO(2-1), ^{12}CO(3-2), and ^{13}CO(1-0) line intensities are represented by black, red, blue, and brown colors, respectively. The arrows show the values with upper limits. SE and NW represent the southeast and northwest parts of the major axis of the galaxies, respectively.

2.2.3. Line ratios

Before obtaining integrated CO intensity line ratios, we should first ensure all the data cubes have the same angular resolution, i.e., the common beam size of 17 arcsecs. We convolved the ^{12}CO(2-1) and ^{12}CO(3-2) data cubes to the common beam using MIRIAD task *convol*. After obtaining all data cubes at the same angular resolution, we extracted the CO spectra from each position in the major axis of the galaxies (see Figure 1). We applied the Gaussian fit to each individual spectrum to obtain the beam-averaged integrated intensities. We finally obtained the line ratios of ^{12}CO(1-0)/^{13}CO(1-0) (hereafter R_{11}), ^{12}CO(2-1)/^{12}CO(1-0) (hereafter R_{21}), and ^{12}CO(3-2)/^{12}CO(1-0) (hereafter R_{31}). The ratios are shown in Figure 4. Figure 4 shows the CO line ratios (i.e., R_{11} (black), R_{21} (red), and R_{31} (blue)) as a function of angular distance over the major axis of NGC 5055 and NGC 3627 galaxies. The data points with an arrow indicate the limit values. Vertical dashed lines on "panel b" represent the center of the galaxy's disc. Spearman correlation coefficients, r_s (Spearman, 1904), were also shown in the panels.

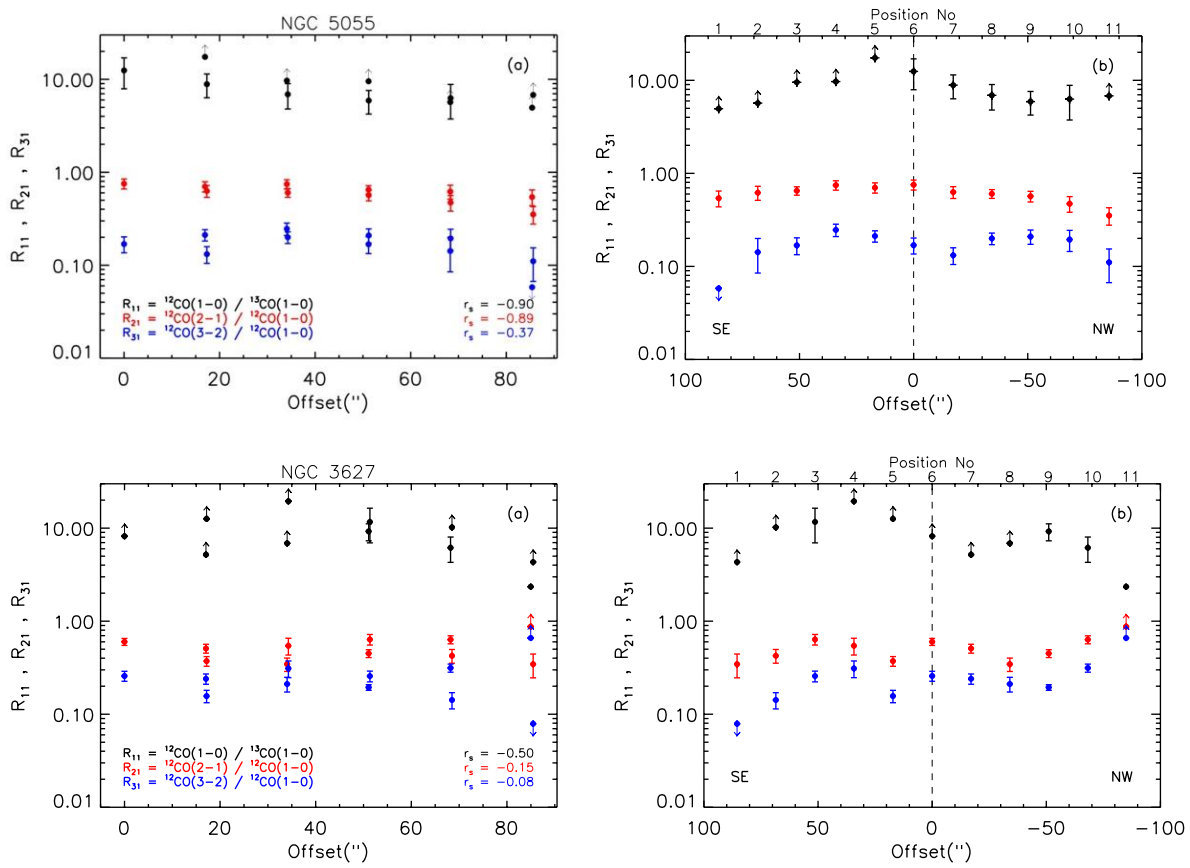

Figure 4. The CO line ratios, i.e., R_{11} (black), R_{21} (red), and R_{31} (blue), in NGC 5055 (top panels) and NGC 3627 (lower panels) are shown as a function of angular distance over the major axis of both galaxies (see Figure 1 for the positions). The data points with an arrow indicate the limit values. Vertical dashed lines on panel b represent the center of the galaxy's disc. Spearman correlation coefficients (r_s), were also estimated and shown in the panels.

3. Results and Discussion

3.1. Moment maps and integrated intensities

The distribution of CO gas in the disc of both galaxies is shown in Figure 1. As seen in Figure 1, NGC 3627 has two prominent gaseous arms and a bar, while the gaseous disc of NGC 5055 is patchy without a prominent bar. There is only one bright CO emission in the center of NGC 5055, while NGC 3627 has three multiple bright spots across its major axis, i.e., the center and two positions on both ends of the bar (Figure 1). The two bright spots at the end of the bar in NGC 3627 could be due to our viewing angle (i.e., the higher the column density, the higher the CO brightness) or CO could be brighter at those positions due to higher star formation activity.

The integrated intensities as a function of radius are shown in Figure 3. The ^{13}CO(1-0) line is the weakest line compared to the others, and it was not detected in the SE (southeastern) part of NGC 5055 and some positions across the disc of NGC 3627. As seen in Figure 3, line intensities decrease from the galaxy's center to the outskirts. The decrease happens more gradually in NGC 5055 compared to NGC 3627, where the line intensities show peaks not only at the center but also at some positions outside the center (i.e., positions 3 and 9, see Figure 3).

This indicates a more heterogeneous distribution of molecular gas in the disc of NGC 3627 compared to NGC 5055. It is also consistent with the bright spots seen at the moment 0 maps of NGC 3627, i.e., the two bright spots outside the central region and along the major axis (see the top-right panel in Figure 1). NGC 3627 has a prominent bar, while NGC 5055 does not. This difference in

morphology could be the reason for the difference in variation of the CO line intensity across the disc of the galaxies.

A higher temperature is required to excite the higher transition of a molecule. Accordingly ^{12}CO(1-0) requires lower average kinetic temperature than ^{12}CO(2-1) and the ^{12}CO(2-1) requires lower temperature than ^{12}CO(3-2) and so on. The ^{12}CO(1-0) intensity at the center of galaxies NGC 5055 and NGC 3627 have approximately the same values within the error bars, i.e., 68.4 ± 6.4 K km s^{-1} and 66.8 ± 5.0 K km s^{-1} for, respectively. The center of NGC 5055 is brighter (51.6 ± 4.1 K km s^{-1}) than NGC 3627 (40.1 ± 1.7 K km s^{-1}) in ^{12}CO(2-1), while the center of NGC 3627 is brighter (17.2 ± 1.7 K km s^{-1}) than NGC 5055 (11.5 ± 1.9 K km s^{-1}) in ^{12}CO(3-2). Overall, NGC 3627 possibly has an ISM with a higher average temperature at its center. This could be that NGC 3627 is hosting an AGN, which could heat the environment in the vicinity and make ^{12}CO(3-2) brighter at its center.

3.2. Line ratios

Probing the line ratios has the potential to provide a clearer insight into the physical properties of the ISM. Since ^{12}CO(1-0) is generally optically thick while its isotopologue ^{13}CO(1-0) is thinner in galaxies, the ratio of R_{11} could give information on the optical depth and the level of star formation activity. The higher R_{11} ratio, therefore, could indicate thinner gas, which could be a result of supernova explosion(s), and/or strong stellar winds, all of which could dissipate the surrounding gas. The ratios between ^{12}CO(1-0) and its higher transitions, such as ^{12}CO(2-1) and ^{12}CO(3-2), provide insights into the average temperature in the ISM, i.e., the higher the R_{21}, and R_{31} ratios, the higher the temperature.

The three R_{11}, R_{21}, and R_{31} line ratios obtained across the disc of both galaxies NGC 5055 and NGC 3627 are shown in Figure 4. Since the ^{12}CO(1-0) is the brightest emission among the lines, all the ratios obtained along the major axis of each galaxy are as follows: $R_{11} > 1$, $R_{21} < 1$, and $R_{31} < 1$ (see Figure 4).

3.2.1. Center

The values of R_{11} ratios at the center of NGC 5055 and NGC 3627 are 4.5 ± 0.7 and 8.2 (lower limit), respectively. The higher R_{11} ratio at the center of NGC 3627 indicates thinner gas than that of NGC 5055. NGC 5055 and NGC 3627 galaxies have very similar R_{21} ratios at their centers, i.e., 0.75 ± 0.09 and 0.60 ± 0.05 , respectively. However, the R_{31} ratio, as an indication of higher temperature, is slightly higher at the center of NGC 3627 (0.26 ± 0.03) than at the center of NGC 5055 (0.17 ± 0.03). All three CO line ratios obtained at the center of the galaxies indicate that NGC 3627 has thinner and slightly hotter gas in its center than NGC 5055.

The low-*J* CO line ratios (R_{11}, R_{21}, and R_{31}) could have different values not only at different types of galaxies but also at different locations over the same galaxy. The gaseous center of spiral galaxies gas has the ratio of $R_{11} > 1$ and generally $5 < R_{11} < 30$ (Israel, 2020). However, starburst galaxies could have $1 < R_{21} < 2$ (Israel, 2020). The R_{31} ratios at the center of spiral galaxies are generally within a range of $0.2 < R_{31} < 0.7$ (Mauersberger et al., 1999). The luminous infrared galaxies mostly have $0.2 < R_{31} < 1.0$ at their centers, whereas the galaxies with AGN have $R_{31} < 1.0$ (Yao et al., 2003; Lamperti et al., 2020; Topal, 2021). As seen in Figure 5, the center of NGC 5055 (i.e., open circle in the figure, respectively) has similar R_{11} line ratios to that observed in the center of spirals (grey-shaded area in Figure 5) and active galaxies (brown stars in Figure 5). However, the center of NGC 3627 (open circle in Figure 5) has a lower R_{11} and R_{21} ratios compared to the center of NGC 5055 (open triangle in Figure 5), and most spirals (cyan-shaded area in Figure 5) as a result of being less bright in ^{12}CO(2-1) (see the central position in the red line in Figure 3). However, please note that R_{11} ratio in the center of NGC 3627 is a lower limit. Additionally, hotter and more compact gas component indicated by ^{12}CO(3-2) transition is brighter in the center of NGC 3627 than in NGC 5055 (see the central position in the blue line in Figure 3). It is, therefore, still possible that the ISM in the central region of NGC 3627 could host a more tenuous and hotter gas component than that in the center of NGC 5055. The central bar in NGC 3627 could play a major role in such complexity by accumulating cold or warm gas to the AGN-hosting central region of NGC 3627.

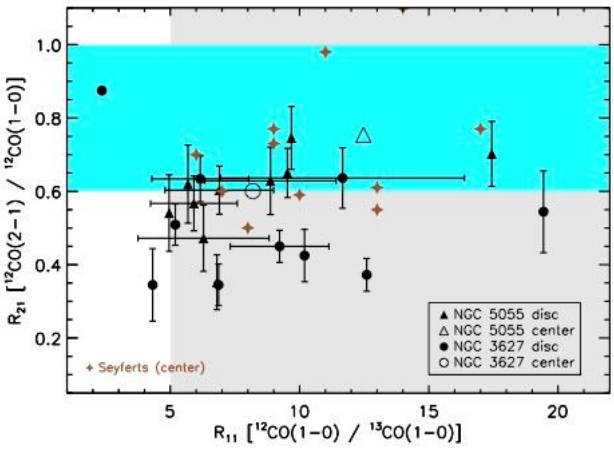

Figure 5. The ratios of the integrated CO line intensities. Black triangles and circles represent the ratios (i.e., R_{11} and R_{21}) in NGC 5055 and NGC 3627, respectively. The ratios in the center of NGC 5055 and NGC 3627 are shown by an open triangle and circle, respectively. Grey and cyan-shaded areas represent the range for the R_{11} ratios detected in the center of nearby spiral galaxies (Israel, 2020) and the R_{21} ratios across the disc of spiral galaxies (Leroy et al., 2009), respectively. The data points without error bars indicate the lower limit values for the line ratios at that position. Brown stars indicate the R_{11} and R_{21} ratios obtained in the central region of Seyfert galaxies (Papadopoulos & Seaquist, 1998).

3.2.2. Along the bar

As seen in Figure 4 (i.e., panel a for both galaxies), the correlation between the line ratios and the distance from the galactic center is negative. The Spearman correlation coefficients were calculated considering only the positions with detections, i.e., no upper limit ratios were considered. The correlation is stronger in NGC 5055 (excluding R_{31} having a weaker correlation), while it is much weaker in NGC 3627, except R_{11} which has a moderate correlation, i.e., r_s = -0.50 (see Figure 4). However, please note that since the correlation found for R_{11} in NGC 3627 and that in NGC 5055 are based on only five (i.e., ^{13}CO(1-0) was detected at only five positions in NGC 3627) and three (i.e., ^{13}CO(1-0) was detected at only three positions in NGC 3627) positions, the correlation between R_{11} and the galactocentric radius is not as statistically significant as the other two line ratios and the radius.

The right panels in Figure 4 show the variation of line ratios on each side of the disc separately. As seen in the figure, the variation is different on each side of the disc. In NGC 5055, R_{11} gradually decreases on both sides of the disc, although it is not clear for the southeastern part of the disc, i.e., the line ratios are all lower limit there. However, after 50 arcsecs (a linear size of $\approx$ 2.2 kpc over the galaxy) from the center in the northwestern part, the ratio tends to increase again. The R_{21} ratio also shows a gradual decrease from the center, but the overall change is small. The R_{31} ratio follows a similar pattern on each side, i.e., the ratio increases up to 30 arcsecs (a linear size of $\approx$ 1.3 kpc) followed by a decrease (see Figure 4). This indicates that the gas gets thinner from the center to the outskirts, while the temperature seems to fluctuate, reaching a peak at about 30 arcsecs from the center, and then decreasing.

In NGC 3627, the line ratios show a more complicated pattern through the disc of the galaxy. There is no strong correlation between the line ratios and the galactocentric distance in NGC 3627 (see the lower panels in Figure 4). For the R_{11}, R_{21}, and R_{31} line ratios, Spearman correlation coefficients are equal to -0.50, -0.15 and -0.08, respectively. The R_{21} and R_{31} ratios decrease from the center to about 30 arcsecs on both sides of the disc. However, while the ratios gradually increase on both sides after about 30 arcsecs, they start to decrease again at 50 arcsecs on the southeastern part of the disc, contrary to a continuous increase on the northwestern part of the disc (see Figure 4). This indicates a difference in temperature variation on each side of the disc.

NGC 3627 shows generally more fluctuations in the line ratios than NGC 5055. This could result from the similar fluctuations seen in the integrated intensities across the disc of the NGC 3627.

As seen from the cyan-shaded area in Figure 5, Milky Way and nearby spiral galaxies have $0.6 < R_{21} < 1$ across their discs (e.g., Leroy et al., 2009; Topal, 2020). Most positions in the disc of both galaxies have lower R_{21} ratios than nearby spirals (cyan-shaded area in Figure 5), indicating lower temperature on average. However, the R_{11} ratios seem similar to other galaxies (grey-shaded area in Figure 5).

4. Conclusion

We probed the gas clouds in two spiral galaxies, NGC 5055 and NGC 3627, using multiple emission lines of low-*J* CO transitions taken from the COMING (Sorai et al., 2019), the HERACLES (Leroy et al., 2009), and the NGLS data (Wilson et al., 2012). The main results are as follows.

^{12}CO(1-0) is the most extensive emission across the disc of both galaxies, while ^{13}CO(1-0) is more centrally concentrated and was not detected at the center of NGC 3627. The CO is the brightest at the center of both galaxies, but NGC 3627 also has two CO-bright spots at both ends of its bar.

The integrated CO intensity decreases from the center to the outskirts in both galaxies. However, NGC 3627 does not show a gradual decrease in the intensity (i.e., showing some peaks at extranuclear positions). This indicates a more heterogeneous gas distribution in NGC 3627 than that of NGC 5055.

The integrated R_{11}, R_{21}, and R_{31} CO line ratios show a negative correlation with the galactocentric distance in both galaxies, i.e., the ratios decrease as the distance from the center increases. However, the correlation along the disc of NGC 5055 is stronger than that seen in NGC 3627. The R_{31} shows the same pattern on each side of the NGC 5055. The ratio increases from the center to about 30 arcsecs and then decreases in the SE and NW parts of the disc. The southeastern part of the NGC 3627 shows a similar trend as in the NGC 5055, while the northeastern of the disc in NGC 3627 shows an opposite trend, i.e., the ratio decreases first and then gradually increases. This indicates different physical properties in the ISM, leading to a different level of star formation activity in each galaxy.

Most positions over the disc of NGC 5055 and NGC 3627 have lower R_{21} but similar R_{11} ratios compared to other galaxies. However, the center of both galaxies has different line ratios. The center of NGC 3627 has lower R_{11} (although R_{11} is a lower limit) and R_{21} ratios compared to the center of NGC 5055, and most spirals. The center of NGC 3627 is brighter in ^{12}CO(3-2) and fainter in ^{12}CO(2-1) transitions compared to the center of NGC 5055, indicating an ISM with a higher average gas kinetic temperature in the center of NGC 3627, but the difference in opacity is not clear. The central bar in NGC 3627 could play an essential role in such complexity by accumulating cold or warm gas in the central region.

Acknowledgments

The authors thank the anonymous referees for their useful comments and suggestions. This research has used the NASA/IPAC Infrared Science Archive, operated by the Jet Propulsion Laboratory, California Institute of Technology, under contract with the National Aeronautics and Space Administration. The James Clerk Maxwell Telescope is operated by the East Asian Observatory on behalf of The National Astronomical Observatory of Japan; Academia Sinica Institute of Astronomy and Astrophysics; the Korea Astronomy and Space Science Institute; the National Astronomical Research Institute of Thailand; Center for Astronomical Mega-Science (as well as the National Key R&D Program of China with No. 2017YFA0402700). Additional funding support is provided by the Science and Technology Facilities Council of the United Kingdom and participating universities and organizations in the United Kingdom and Canada. This publication made use of data from COMING, CO Multi-line Imaging of Nearby Galaxies, a legacy project of the Nobeyama 45-m radio telescope.

References

Cappellari, M., Emsellem, E., Krajnović, D., McDermid, R. M., Serra, P., Alatalo, K., ..., & Young, L. M. (2011). The ATLAS3D project–VII. A new look at the morphology of nearby galaxies: the kinematic morphology–density relation. *Monthly Notices of the Royal Astronomical Society*, 416(3), 1680-1696. doi:10.1111/j.1365-2966.2011.18600.x

de Vaucouleurs, G. (1974). Structure, dynamics and statistical properties of galaxies. *Symposium* -

International Astronomical Union, 58, 1-53. doi:10.1017/S007418090002430X

de Vaucouleurs, G., de Vaucouleurs, A., Corwin, Jr. H. G., Buta, R. J., Paturel, G., Fouque, P. (1991). *Third Reference Catalogue of Bright Galaxies. Volume I: Explanations and references. Volume II: Data for galaxies between 0h and 12h. Volume III: Data for galaxies between 12h and 24h.* New York, USA: Springer.

Endres, C. P., Schlemmer, S., Schilke, P., Stutzki, J., & Müller, H. S. (2016). The cologne database for molecular spectroscopy, CDMS, in the virtual atomic and molecular data centre, VAMDC. *Journal of Molecular Spectroscopy*, 327, 95-104. doi:10.1016/j.jms.2016.03.005

Fukui, Y., Kawamura, A., Wong, T., Murai, M., Iritani, H., Mizuno, N., ..., & Kim, S. (2009). Molecular and atomic gas in the large magellanic cloud. II. Three-dimensional correlation between CO and H I. *The Astrophysical Journal*, 705(1), 144. doi:10.1088/0004-637X/705/1/144

Hollenbach, D. J., & Tielens, A. G. G. M. (1999). Photodissociation regions in the interstellar medium of galaxies. *Reviews of Modern Physics*, 71(1), 173. doi:10.1103/RevModPhys.71.173

Hubble, E. P. (1936). *Realm of the Nebulae*. USA: Yale University Press.

Israel, F. P. (2020). Central molecular zones in galaxies: 12CO-to-13CO ratios, carbon budget, and X factors. *Astronomy & Astrophysics*, 635, A131. doi:10.1051/0004-6361/201834198

Kormendy, J., & Bender, R. (2012). A Revised parallel-sequence morphological classification of galaxies: structure and formation of S0 and spheroidal galaxies. *The Astrophysical Journal Supplement Series*, 198, 2-41. doi:10.1088/0067-0049/198/1/2

Lamperti, I., Saintonge, A., Koss, M., Viti, S., Wilson, C. D., He, H., ..., & Tacconi, L. J. (2020). The CO (3–2)/CO (1–0) luminosity line ratio in nearby star-forming galaxies and active galactic nuclei from xCOLD GASS, BASS, and SLUGS. *The Astrophysical Journal*, 889(2), 103. doi:10.3847/1538-4357/ab6221

Leroy, A. K., Walter, F., Bigiel, F., Usero, A., Weiss, A., Brinks, E., ..., & Roussel, H. (2009). Heracles: The HERA CO line extragalactic survey. *The Astronomical Journal*, 137(6), 4670. doi:10.1088/0004-6256/137/6/4670

Makarov, D., Prugniel, P., Terekhova, N., Courtois, H., & Vauglin, I. (2014). HyperLEDA. III. The catalogue of extragalactic distances. *Astronomy & Astrophysics*, 570, A13. doi:10.1051/0004-6361/201423496

Maloney, P. R., Hollenbach, D. J., & Tielens, A. G. G. M. (1996). X-Ray--irradiated molecular gas. I. physical processes and general results. *Astrophysical Journal*, 466, 561-584.

Markwardt, C. B. (2009, November). Non-linear least squares fitting in IDL with MPFIT. Astronomical Data Analysis Software and Systems XVIII, ASP Conference Series. Quebec, Canada. doi:10.48550/arXiv.0902.2850

Mauersberger, R., Henkel, C., Walsh, W., & Schulz, A. (1999). Dense gas in nearby galaxies. XII. A survey for CO J=3-2 emission. *Astronomy and Astrophysics*, 341, 256-263.

McKee, C. P., & Hollenbach, D. J. (1980). Interstellar shock waves. *Annual Review of Astronomy and Astrophysics*, 18(1), 219-262. doi:10.1146/annurev.aa.18.090180.001251

Padovani, M., Galli, D., & Glassgold, A. E. (2009). Cosmic-ray ionization of molecular clouds. *Astronomy & Astrophysics*, 501(2), 619-631. doi:10.1051/0004-6361/200911794

Paglione, T. A., Wall, W. F., Young, J. S., Heyer, M. H., Richard, M., Goldstein, M., ..., & Perry, G. (2001). A mapping survey of the 13CO and 12CO emission in galaxies. *The Astrophysical Journal Supplement Series*, 135(2), 183. doi:10.1086/321785

Papadopoulos, P. P., & Seaquist, E. R. (1998). Physical conditions of the molecular gas in Seyfert galaxies. *The Astrophysical Journal*, 492(2), 521. doi:10.1086/305052

Saintonge, A., & Catinella, B. (2022). The cold interstellar medium of galaxies in the local universe. *Annual Review of Astronomy and Astrophysics*, 60, 319-361. doi:10.1146/annurev-astro-021022-043545

Sault, R. J., Teuben, P. J., & Wright, M. C. H. (1995). A retrospective view of Miriad. Astronomical Data Analysis Software and Systems IV, ASP Conference Series. San Francisco, USA. doi:10.48550/arXiv.astro-ph/0612759

Sorai, K., Kuno, N., Muraoka, K., Miyamoto, Y., Kaneko, H., Nakanishi, H., ..., & Saita, C. (2019). CO Multi-line Imaging of Nearby Galaxies (COMING). IV. Overview of the project. *Publications of the Astronomical Society of Japan*, 71, S14.doi:10.1093/pasj/psz115

Spearman, C. (1904). The proof and measurement of association between two things, *The American Journal of Psychology*. 15, 72-101. doi:10.2307/1412159

Topal, S., Bureau, M., Davis, T. A., Krips, M., Young, L. M., & Crocker, A. F. (2016). Molecular gas kinematics and line diagnostics in early-type galaxies: NGC 4710 and NGC 5866. *Monthly Notices of the Royal Astronomical Society*, 463(4), 4121-4152. doi:10.1093/mnras/stw2257

Topal, S. (2020). Molecular line ratio diagnostics along the radial cut and dusty ultraviolet-bright clumps in a spiral galaxy NGC 0628. *Monthly Notices of the Royal Astronomical Society*, 495(3), 2682-2712. doi:10.1093/mnras/staa1146

Topal, S. (2021). Molecular line ratio diagnostics and gas kinematics in the AGN host Seyfert galaxy NGC 5033. *Monthly Notices of the Royal Astronomical Society*, 504(4), 5941-5953. doi:10.1093/mnras/stab1269

Weinreb, S., Barrett, A. H., Meeks, M. L., & Henry, J. C. (1963). Radio observations of OH in the interstellar medium. *Nature*, 200, 829-831. doi:10.1038/200829a0

Wilson, C. D., Warren, B. E., Israel, F. P., Serjeant, S., Attewell, D., Bendo, G. J., ..., & White, G. J. (2012). The JCMT nearby galaxies legacy survey—VIII. CO data and the LCO (3-2)-LFIR correlation in the SINGS sample. *Monthly Notices of the Royal Astronomical Society*, 424(4), 3050-3080. doi:10.1111/j.1365-2966.2012.21453.x

Yao, L., Seaquist, E. R., Kuno, N., & Dunne, L. (2003). CO molecular gas in infrared-luminous galaxies. *The Astrophysical Journal*, 588(2), 771. doi:10.1086/374333